Inorganic Chemistry

ARTICLE

pubs.acs.org/IC

Two-Electron Oxidation of Deoxyguanosine by a Ru(III) Complex without Involving Oxygen Molecules through Disproportionation

Sunhee Choi,* DaWeon Ryu, Joseph G. DellaRocca, Matthew W. Wolf, and Justin A. Bogart

Department of Chemistry and Biochemistry, Middlebury College, Middlebury, Vermont 05753, United States

Supporting Information

ABSTRACT: Among the many mechanisms for the oxidation of guanine derivatives (G) assisted by transition metals, Ru^{III} and Pt^{IV} metal ions share basically the same principle. Both Ru^{III}- and Pt^{IV}-bound G have highly positively polarized C8−H's that are susceptible to deprotonation by OH^-, and both undergo two-electron redox reactions. The main difference is that, unlike Pt^{IV}, Ru^{III} is thought to require O_2 to undergo such a reaction. In this study, however, we report that $[Ru^{III}(NH_3)_5(dGuo)]$ (dGuo = deoxyguanosine) yields cyclic-5′-O-C8-dGuo (a two-electron G oxidized product, cyclic-dGuo) without O_2. In the presence of O_2, 8-oxo-dGuo and cyclic-dGuo were observed. Both $[Ru^{II}(NH_3)_5(dGuo)]$ and cyclic-dGuo were produced from $[Ru^{III}(NH_3)_5(dGuo)]$ accelerated by $[OH^-]$. We propose that $[Ru^{III}(NH_3)_5(dGuo)]$ disproportionates to $[Ru^{II}(NH_3)_5(dGuo)]$ and $[Ru^{IV}(NH_3)_4(NH_2^-)(dGuo)]$, followed by a 5′-OH attack on C8 in $[Ru^{IV}(NH_3)_4(NH_2^-)(dGuo)]$ to initiate an intramolecular two-electron transfer from dGuo to Ru^{IV}, generating cyclic-dGuo and Ru^{II} without involving O_2.

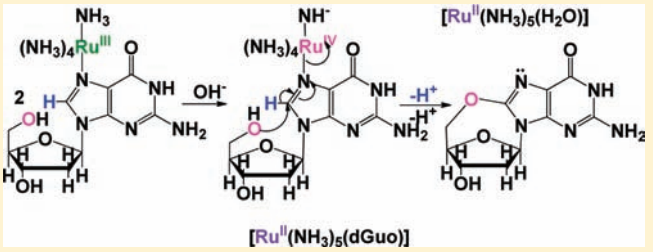

INTRODUCTION

Oxidation of DNA is a common cause of mutation, cancer, aging, and death.[1] Many transition metal complexes of V, Cr, Mn, Co, Ni, Cu, Ru, Rh, Re, Os, and Pt are known to promote DNA oxidation.[2] Among the many mechanisms for the oxidation of purine derivatives assisted by transition metals, Ru^{III} and Pt^{IV} metal ions share basically the same principle. Ru^{III} and Pt^{IV} complexes bind to N7 of the guanine derivatives (G) to form $[Ru^{III}$-G] and $[Pt^{IV}$-G], respectively. Clarke's group has shown that for $[Ru^{III}(NH_3)_5(L)]$ (L = dGuo, Ino, 1-MeIno), the intermolecular nucleophilic attack to C8 by OH^- in solution initiates a two-electron transfer from G to Ru^{III} and O_2 to produce $[Ru^{III}$-(8-oxo-G)].[3] Our group has demonstrated that for Pt^{IV}-G, both intramolecular (5′-OH and 5′-phosphate)[4a,b] and intermolecular (OH^- and phosphate in solution)[4c] nucleophilic attacks occur at C8 followed by a two-electron transfer from G to Pt^{IV}. While 8-oxo-G was the oxidation product of G by the 5′-phosphate intramolecular nucleophile[4a] and the intermolecular nucleophiles (OH^- and phosphate),[4c] cyclic-5′-O-C8-3′dGMP was the oxidation product from the 5′-OH intramolecular nucleophile.[4b]

In 1971, Taube's group first reported the disproportionation of $[Ru^{III}(NH_3)_5(py)]$ complexes in basic solution to $[Ru^{II}(NH_3)_5(py)]$ and $[Ru^{IV}(NH_3)_5(py)]$.[5] Their discovery was based on the observation that a solution containing $[Ru^{III}(NH_3)_5(py)]$ complexes, which was colorless, developed a strong color when its pH was raised to 8 or above. They attributed the color to the charge-transfer band (407 nm) of $[Ru^{II}(NH_3)_5(py)]$ complexes. Since the conversion of $[Ru^{III}(NH_3)_5(py)]$ to $[Ru^{II}(NH_3)_5(py)]$ never exceeded 50% of the initial $[Ru^{III}(NH_3)_5(py)]$, the other 50% of the product was speculated to be $[Ru^{IV}(NH_3)_5(py)]$. New visible bands at 524 nm (arsenate buffer) and at 558 nm (carbonate buffer) were proposed to arise from $[Ru^{IV}(NH_3)_5(py)]$.

Later, Clarke's group also reported the disproportionation of *trans*-$[Ru^{III}(NH_3)_4(py)(L)]$ (L = Ino, 1-MeIno, Guo, dGuo) to the corresponding Ru^{II} and Ru^{IV} species.[6] Like $[Ru^{III}(NH_3)_5(py)]$, *trans*-$[Ru^{III}(NH_3)_4(py)(L)]$ in basic solution developed a strong charge-transfer band at 413 nm, which was attributed to the formation of *trans*-$[Ru^{II}(NH_3)_4(py)(L)]$. Although they could not isolate *trans*-$[Ru^{II}(NH_3)_4(py)(L)]$, the evidence of the formation of Ru^{II} strongly indicated the simultaneous formation of Ru^{IV}. The deprotonation of an ammine species was suggested to be the rate-limiting step in disproportionation.

For *trans*-$[Ru^{III}(NH_3)_4(py)(Guo)]$ in basic solution, the disproportionation was followed by the formation of *trans*-$[Ru^{III}(NH_3)_4(py)(Gua)]$ and free ribose.[6a] The cleavage of the N-glycosidic bond from *trans*-$[Ru^{IV}(NH_3)_4(py)(Guo)]$ took place at high pH to yield *trans*-$[Ru^{III}(NH_3)_4(py)(Gua)]$ and free ribose. Glycolysis was more efficient at high pH. The ratios of *trans*-$[Ru^{III}(NH_3)_4(py)(Gua)]$ to *trans*-$[Ru^{III}(NH_3)_4(py)(Guo)]$ were 1:7 and 1:11 at pH 11 and pH 9, respectively.

The objective of this work was to investigate the redox and disproportionation behavior of $[Ru^{III}(NH_3)_5(dGuo)]$ to test whether the oxidation of G by intramolecular attack observed with Pt^{IV} complexes could be extended to Ru^{III} complexes, and to test whether $[Ru^{III}(NH_3)_5(dGuo)]$ undergoes disproportionation like $[Ru^{III}(NH_3)_4(py)(dGuo)]$. Analysis of the reaction products of $[Ru^{III}(NH_3)_5(dGuo)]$ at high pH suggested disproportionation was followed by a redox reaction.

Received: February 18, 2011
Published: June 16, 2011

dx.doi.org/10.1021/ic2003518 | *Inorg. Chem.* 2011, 50, 6567–6574

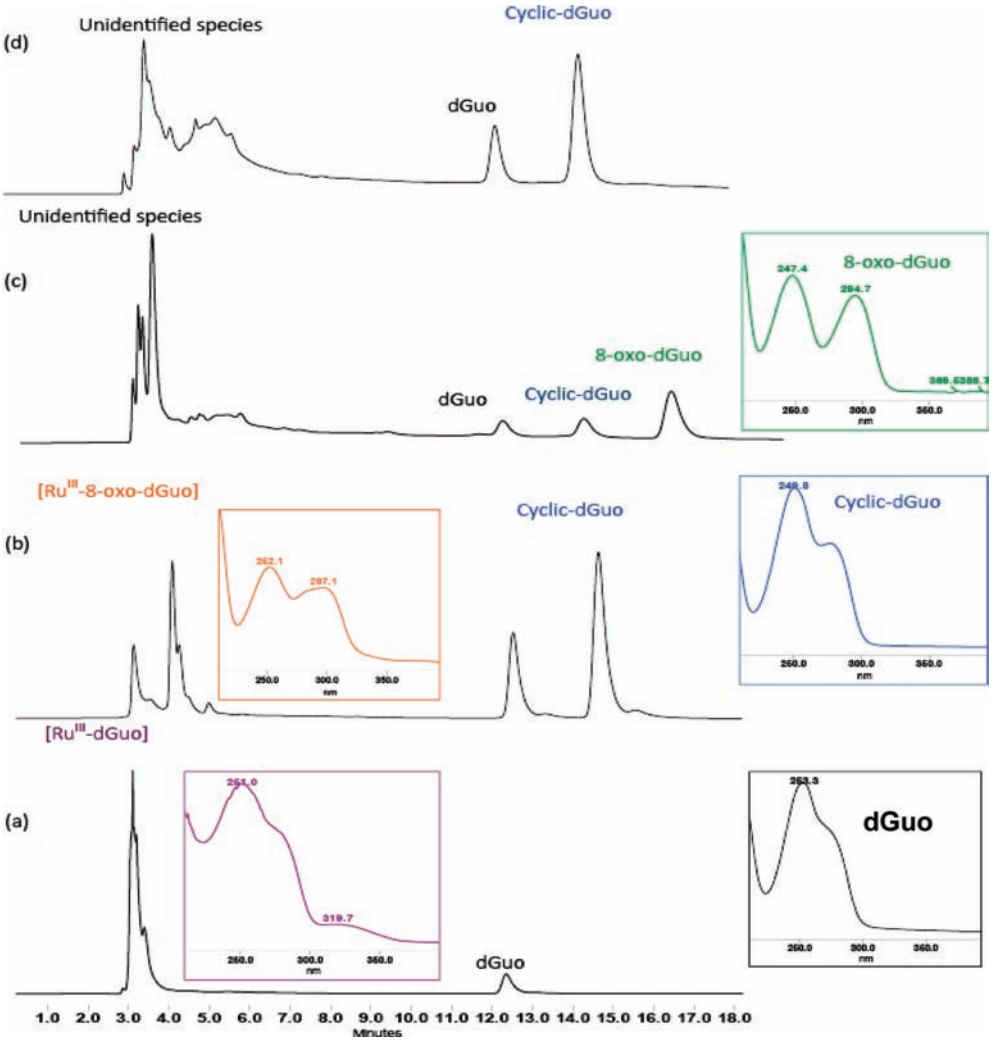

Figure 1. HPLC chromatograms of $[Ru^{III}(NH_3)_5(dGuo)]$ (a) at pH 6.7 and $t = 0$, (b) under O_2 at $t = 12$ h, (c) after reducing the solution at $t = 12$ h under O_2 with Zn/Hg, (d) before and after reducing (with Zn/Hg) the reaction solution under Ar at $t = 12$ h. All solutions except (a) were at pH 11.7 and 25 °C. $\lambda_{obs} = 254$ nm. Insets: UV spectra obtained from the HPLC DAD of the corresponding peaks.

RESULTS

Identification of Oxidation Products of $[Ru^{III}(NH_3)_5$-(dGuo)]. *$[Ru^{III}(NH_3)_5(8\text{-oxo-dGuo})]$.* The HPLC chromatograms of the initial $[Ru^{III}(NH_3)_5(dGuo)]$ product at pH 6.7 and that at pH 11.7 after 12 h under O_2 at 25 °C are shown in Figure 1a and b, respectively. The new peak from the reaction under O_2 at the retention time of 4.5 min is identified as $[Ru^{III}(NH_3)_5(8\text{-oxo-dGuo})]$. The UV spectrum of $[Ru^{III}(NH_3)_5(8\text{-oxo-dGuo})]$ has characteristic absorption maxima at 252 and 297 nm compared to those of $[Ru^{III}(NH_3)_5(dGuo)]$ at 251 nm with a ~280 nm shoulder. The mass spectrum of $[Ru^{III}(NH_3)_5(8\text{-oxo-dGuo})]$ shows isotope clusters of ruthenium (Figure 2b). The cluster with a mass peak of 468.1 m/z, which was not observed prior to the oxidation reaction (Figure 2a), closely matches the exact mass of $[Ru^{III}(NH_3)_5(8\text{-oxo-dGuo})]$ (469.12 g/mol) minus H^+.

The identity of the oxidation product, $[Ru^{III}(NH_3)_5(8\text{-oxo-dGuo})]$, was further confirmed by reducing the complex with Zn/Hg under Ar. The HPLC chromatogram of the reduced solution shows a new peak at a retention time of 17.3 min (Figure 1c). On basis of its HPLC photodiode array detector (DAD) spectrum, which has a characteristic double hump at λ_{max} 247 and 294 nm, it was identified as 8-oxo-dGuo. It was also detected by LC/MS at m/z 284.0 (Figure 2c) as a protonated form.

The reaction mixture under Ar after 12 h of reaction at pH 11.7 only contained cylic-G and did not contain $[Ru^{III}(NH_3)_5(8\text{-oxo-dGuo})]$ (Figure 1d). Furthermore, the HPLC chromatogram of the solution after it was reduced by Zn/Hg was basically the same as before the reduction (Figure 1d). The reaction under Ar did not produce 8-oxo-G. This confirms that under an Ar atmosphere, $[Ru^{III}(NH_3)_5(8\text{-oxo-dGuo})]$ was not formed. The reaction mixture at pH 6.7 under O_2 did not contain $[Ru^{III}(NH_3)_5(8\text{-oxo-dGuo})]$ or 8-oxo-dGuo after it was reduced by Zn/Hg. In summary, both OH^- and O_2 are necessary for the generation of $[Ru^{III}(NH_3)_5(8\text{-oxo-dGuo})]$.

Cyclic-(5′-O-C8)-dGuo (cyclic-dGuo). The new peak at a retention time of 14.8 min from the reaction under either O_2 (Figure 1b) or Ar (Figure 1d) is identified as cyclic-dGuo. The UV spectrum of cyclic-dGuo has two distinct peaks at ~250 and ~280 nm compared to that of dGuo, which has the 280 nm peak on the shoulder of the 253 nm peak.[7] This was also true of cyclic-3′-dGMP, the oxidation product of Pt^{IV}-3′-dGMP;[4b] cyclic-3′-dGMP has the distinct ~280 nm peak while 3′-dGMP has the

dx.doi.org/10.1021/ic2003518 |*Inorg. Chem.* 2011, 50, 6567–6574

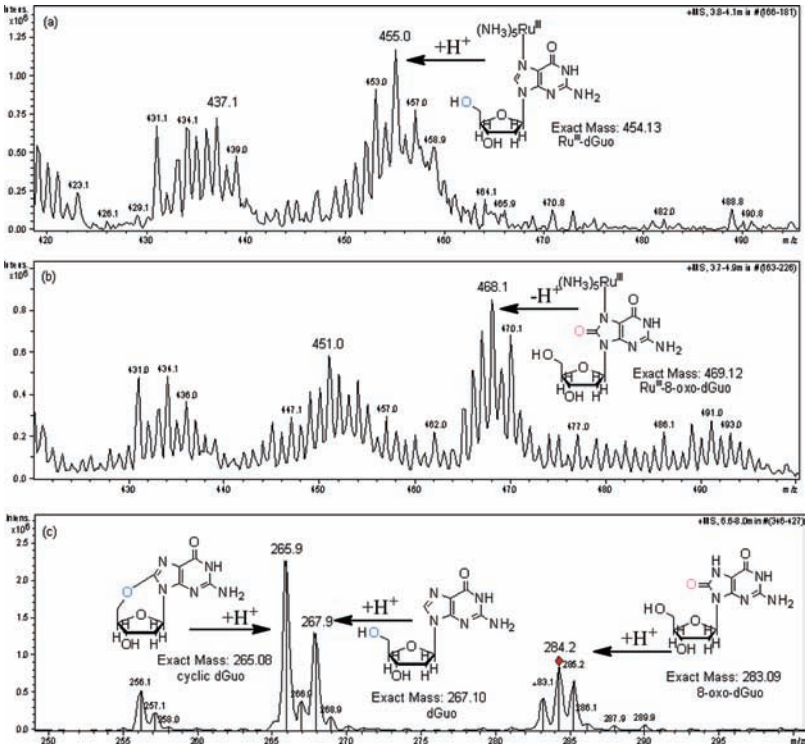

Figure 2. Mass spectra showing (a) $[Ru^{III}(NH_3)_5(dGuo)$ at $t = 0$; (b) $[Ru^{III}(NH_3)_5(8\text{-oxo-dGuo})]$ from the solution of $[Ru^{III}(NH_3)_5(dGuo)]$ at pH 11.7 under O_2 at $t = 12$ h and 25 °C; (c) cyclic-dGuo, dGuo, and 8-oxo-dGuo after reducing solution b with Zn/Hg.

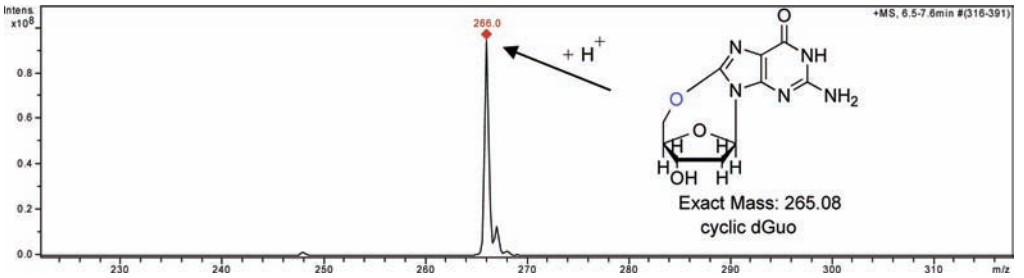

Figure 3. Mass spectrum of cyclic-dGuo isolated by HPLC from the $[Ru^{III}(NH_3)_5(dGuo)]$ reaction mixtures.

280 nm peak on the shoulder of the 250 nm peak. The MS spectrum of the reaction mixture also showed the m/z 266 peak corresponding to a protonated cyclic-dGuo (Figure 2c).

To further confirm the structure of cyclic-dGuo, the fraction corresponding to a 14.8 min HPLC retention time was manually collected and characterized using LC/MS and ^{1}H NMR. The LC/MS spectrum showed one clear peak of 266.0 m/z corresponding to a protonated cyclic-dGuo (Figure 3).

Figure 4 compares the ^{1}H NMR spectra of pure dGuo and cyclic-dGuo. The peaks due to H1′ and H5′ respectively appear at 6.3 and 3.8 ppm for free dGuo but at 6.48 and 4.2 ppm for cyclic-dGuo. The multiple peaks at 3.8 ppm are due to the overlap of the 5′-OH peak in free dGuo, which does not exist in cyclic-dGuo. The doublet feature of the H1′ peak for cyclic-dGuo compared to the triplet for free dGuo further confirms the structure of cyclic-dGuo. In dGuo, there is a free rotation from the 2′-exo, 3′-endo to the 2′-endo, 3′-exo conformation. This allows the H1′ proton to couple with both H2′ protons, giving a triplet peak. However, the formation of the cycle prohibits this rotation, locking the dihedral angles between H1′ and H2′. The dihedral angles around 85° give a zero coupling constant according to the Karplus correlation,[8] which is the reason why H1′ couples with only one of the H2′ protons, giving a doublet. This doublet feature of H1′ was also observed in cyclic-3′-dGMP.[4b] Furthermore, the peak at 7.88 ppm corresponding to H8 of dGuo is absent in the ^{1}H NMR spectrum of cyclic-dGuo, which is consistent with the structure of cyclic-dGuo.

Oxidation Products of [Ru^{III}(NH$_3$)$_5$(dGuo)] in H$_2$^{18}O. $[Ru^{III}(NH_3)_5(dGuo)]$ was synthesized in $H_2{}^{18}O$ (50%). The pH of the reaction solution was raised to pH 11, and O_2 was bubbled through the solution overnight. An HPLC chromatogram confirmed the formation of $[Ru^{III}(NH_3)_5(8\text{-oxo-dGuo})]$ the next day. The solution was reduced by Zn/Hg and analyzed by LC/MS (Figure 5).

The mass spectrum shows peaks of m/z 266.0 and m/z 284.0, which correspond to the protonated cyclic-dGuo (exact mass = 265.08 g/mol) and 8-oxo-dGuo (exact mass = 283.09 g/mol), respectively. A new mass peak of m/z 286.0, which was not observed when the reaction was run in normal $H_2{}^{16}O$ (100%), was identified as 8-^{18}oxo-dGuo. Since 8-^{18}oxo-dGuo resulted

dx.doi.org/10.1021/ic2003518 |*Inorg. Chem.* 2011, 50, 6567–6574

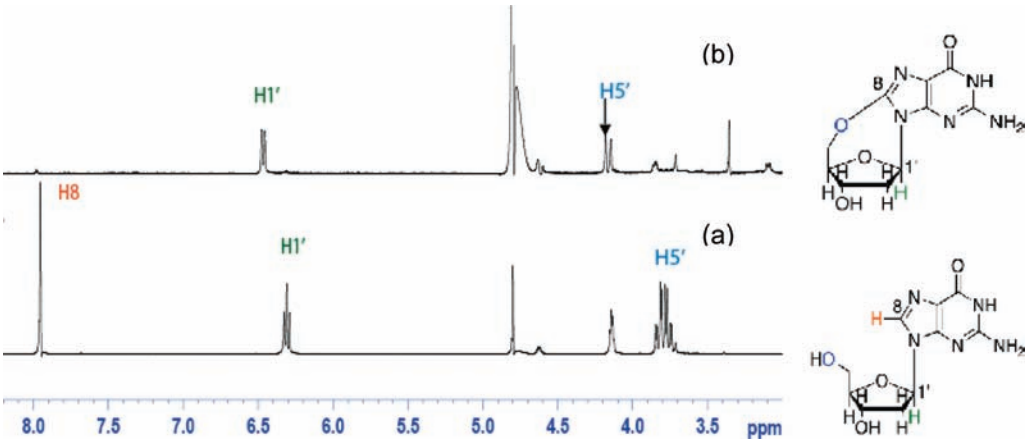

Figure 4. ^{1}H NMR spectra of (a) pure dGuo and (b) cyclic-dGuo in D_2O isolated by HPLC from the $[Ru^{III}(NH_3)_5(dGuo)]$ reaction mixture at pH 11.

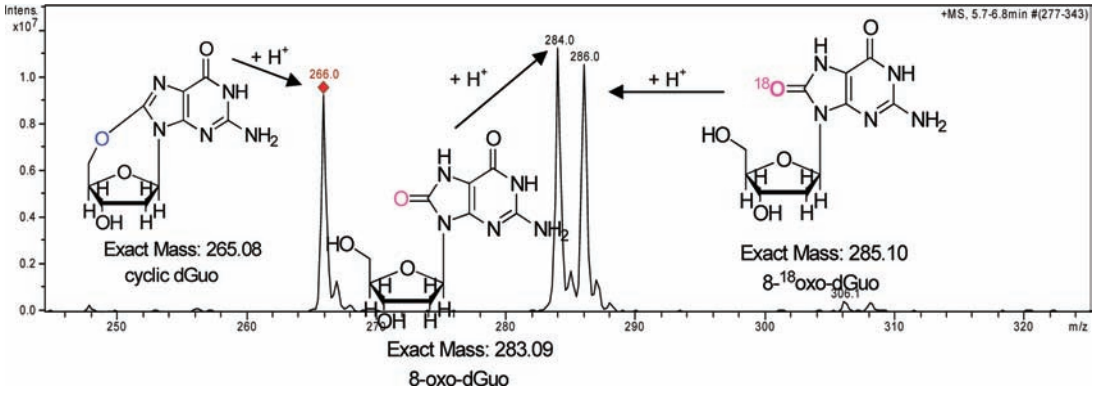

Figure 5. Mass spectrum showing $[cyclic\text{-}dGuo]H^+$, $[8\text{-}oxo\text{-}dGuo]H^+$, and $[8\text{-}^{18}oxo\text{-}dGuo]H^+$ from the $[Ru^{III}(NH_3)_5(dGuo)]$ reaction in $H_2{}^{18}O$ at pH 11 under O_2 for 24 h at 25 °C followed by Zn/Hg reduction.

from an intermolecular attack of $^{18}OH^-$, its mass is +2 mass units heavier than that of 8-^{16}oxo-dGuo. The mass of cyclic-dGuo remained the same, confirming that the source of C8-oxygen in cyclic-dGuo was not from the solvent.

Kinetics of Production of Cyclic-dGuo at Different pH. The concentration of cyclic-dGuo from the solution of $[Ru^{III}(NH_3)_5(dGuo)]$ under Ar over time was monitored by HPLC (Figure 6a). As time progresses, the area of the peak at 14.5 min due to cyclic-dGuo grows to reach a maximum. The concentrations of cyclic-dGuo generated from the $[Ru^{III}(NH_3)_5(dGuo)]$ reactions at pH 10.8 and 10.1 under Ar over time were obtained from the relative peak areas of cyclic-dGuo compared to an internal standard (inosine; Figure 6a). They are displayed in Figure 6b. It clearly shows that cyclic-dGuo was produced faster at pH 10.8 than at pH 10.1. The production of cyclic-dGuo follows the first-order rate law, and the first order rate constant, k_{cycle}, was obtained from the kinetic curve. The k_{cycle} values at 25 °C were determined to be 5.9 (±0.7) × 10^{-4} s^{-1} and 3.2 (±0.2) × 10^{-4} s^{-1} at pH 10.8 and 10.1, respectively.

Kinetics of Production of $[Ru^{II}(NH_3)_5(dGuo)]$. The production rate of $[Ru^{II}(NH_3)_5(dGuo)]$ from $[Ru^{III}(NH_3)_5(dGuo)]$ in 100 mM NaCl at 25 °C was studied under Ar using UV−vis spectroscopy (Figure 7). As time progresses, a shoulder around 354 nm increases, and the broad band at 618 nm shifts to 567 nm. The band at 354 nm is assigned to $[Ru^{II}(NH_3)_5(dGuo)]$ (Figure S1, Supporting Information) arising from a metal-to-ligand charge transfer.[5] The broad band at 618 nm is due to $[Ru^{III}(NH_3)_5(dGuo)]$ arising from a charge transfer from a π orbital in G to an empty Ru^{III} t_{2g} orbital.[6a] Taube and Rudd attributed the new band around 558 nm to $[Ru^{IV}(NH_3)_5(py)]$ in a carbonate buffer since no bands are expected from Ru^{II} and Ru^{III} in this region.[5] Therefore, we attribute our 567 nm band to $[Ru^{IV}(NH_3)_5(dGuo)]$.

Kinetic Data Analysis of Disproportionation of $[Ru^{III}(NH_3)_5(dGuo)]$ to $[Ru^{III}(NH_3)_5(dGuo)]$ and $[Ru^{IV}(NH_3)_5(dGuo)]$. Although no $[Ru^{IV}(NH_3)_5(dGuo)]$ was detected or characterized, generation of $[Ru^{II}(NH_3)_5(dGuo)]$ without any reductant was interpreted as the disproportionation of $[Ru^{III}(NH_3)_5(dGuo)]$ to $[Ru^{II}(NH_3)_5(dGuo)]$ and $[Ru^{IV}(NH_3)_5(dGuo)]$ following Taube and Rudd's and Clarke et al.'s studies on $[Ru^{III}(NH_3)_5(py)]$[5] and $[Ru^{III}(NH_3)_4(py)(Guo)]$,[6] respectively. Therefore, the kinetic curve of the generation of $[Ru^{II}(NH_3)_5(dGuo)]$ in Figure 7b is interpreted as the kinetic curve of disproportionation. The rate constants, k_{obs}, of disproportionation at various pH's were obtained by fitting the kinetic curve to eq 1.

$$A_{354} = A_o + (A_\infty - A_o)(1 - e^{-k_{obs}t}) \quad (1)$$

Dependence of Disproportionation on $[OH^-]$ under Ar. The first order rate constants, k_{obs}, for disproportionation under Ar were obtained at different OH^- concentrations and plotted in Figure 8. It shows that the disproportionation rate constant is linearly proportional to the OH^- concentration. The observed rate constant, k_{obs}, is expressed as $k_o + k_1[OH^-]$. The k_o and k_1

dx.doi.org/10.1021/ic2003518 |Inorg. Chem. 2011, 50, 6567–6574

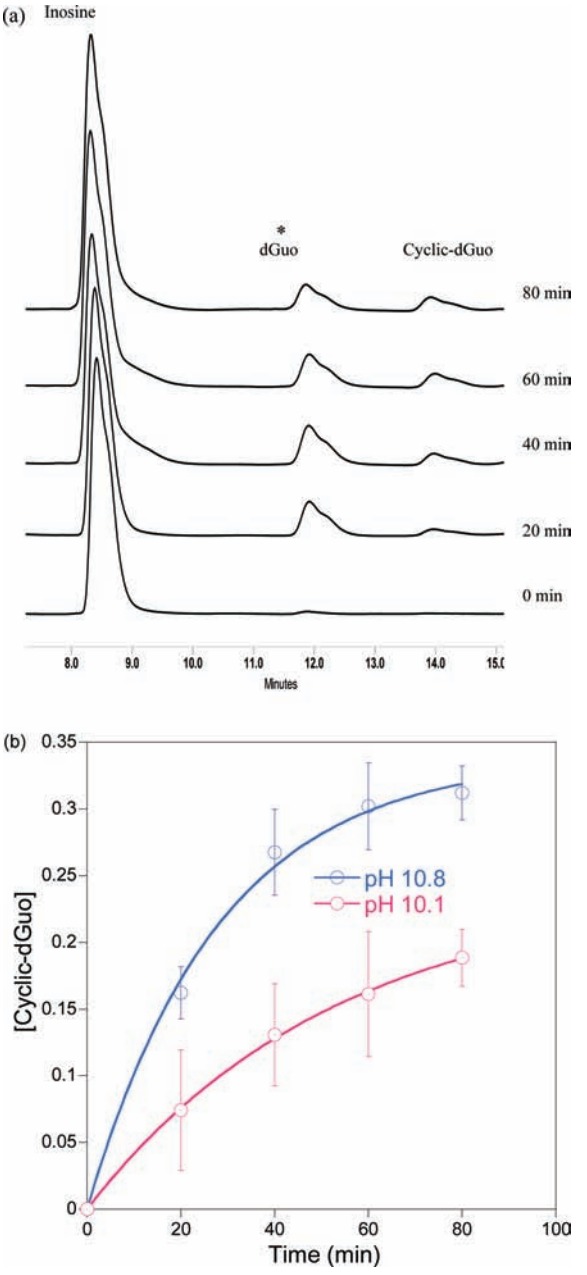

Figure 6. (a) HPLC chromatograms (DAD $\lambda = 260$ nm) of the reaction of $[Ru^{III}(NH_3)_5(dGuo)]$ in a 100 mM NaCl, pH 10.8 solution under Ar. *Some of the $[Ru^{III}(NH_3)_5(dGuo)]$ was degraded to produce free dGuo as soon as the pH of the solution was raised. (b) Overlay of [cyclic-dGuo] vs time at pH 10.8 and 10.1. The theoretical fitted curves giving first-order rate constants of cyclization (k_{cycle}) of 5.9 ($\pm$0.7) $\times$ 10^{-4} s^{-1} at pH 10.8 and 3.2 ($\pm$0.2) $\times$ 10^{-4} s^{-1} at pH 10.1 are drawn with blue and pink curves, respectively.

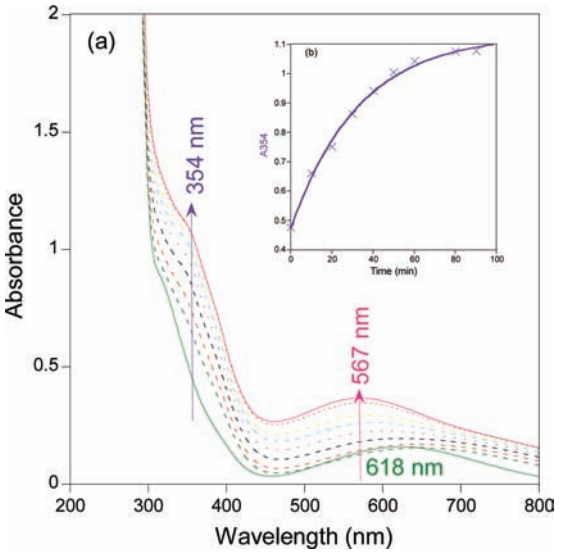

Figure 7. (a) UV−vis scanning kinetics of $[Ru^{III}(NH_3)_5(dGuo)]$ (0.5 mM) in a 100 mM NaCl, pH 9.3 solution at 37 °C, using a 1 cm cuvette. (b) $A_{354\ nm}$ vs time (min). The theoretical fitted curve giving the first-order rate constant k_{obs} of 5.1 $\times$ 10^{-4} s^{-1} is drawn in purple.

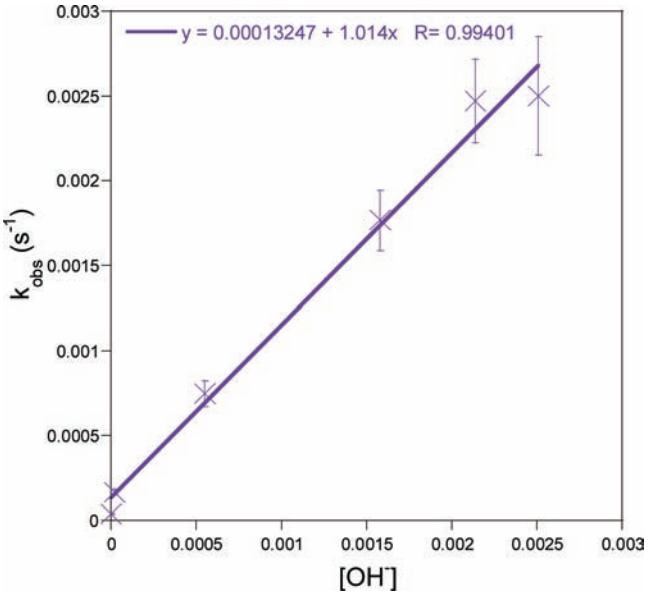

Figure 8. Plot of k_{obs} vs [OH^-] for the disproportionation of $[Ru^{III}(NH_3)_5(dGuo)]$ in 100 mM NaCl at 25 °C.

of $[Ru^{III}(NH_3)_5(dGuo)]$ disproportionation are 1.3 ($\pm$0.8) $\times$ 10^{-4} s^{-1} and 1.0 $\pm$ 0.06 M^{-1} s^{-1}, respectively.

DISCUSSION

At high pH and under O_2, we observed two oxidation products, $[Ru^{III}(NH_3)_5(8\text{-oxo-dGuo})]$ and cyclic-dGuo. But under Ar, only one major oxidation product, cyclic-dGuo, was observed. In terms of $[Ru^{III}(NH_3)_5(8\text{-oxo-dGuo})]$, our results are in accordance with Clarke's proposed mechanism: OH^- in the solvent attacks C8, releasing H−C8, and O_2 is required to form $[Ru^{III}(NH_3)_5(8\text{-oxo-dGuo})]$.[3]

The discovery of cyclic-dGuo is new. Unlike $[Ru^{III}(NH_3)_5(8\text{-oxo-dGuo})]$, the formation of cyclic-dGuo did not depend on the presence of O_2 or require a high concentration of OH^-. Not only was cyclic-dGuo observed under Ar, it was also observed at pH 6.7 after one week (Figure S2, Supporting Information) of reaction in the dark at room temperature. Cyclic-dGuo was always found to be uncomplexed, whereas 8-oxo-dGuo was always found to be bound to Ru^{III}. Since cyclic-dGuo was formed under Ar without any O_2 and it is a two-electron oxidation product, it could not have been formed from a Ru^{III} species, which can only accept one electron.

dx.doi.org/10.1021/ic2003518 |Inorg. Chem. 2011, 50, 6567–6574

Scheme 1. Proposed Mechanism for the Oxidation of dGuo in $[Ru^{III}(NH_3)_5(dGuo)]$[a]

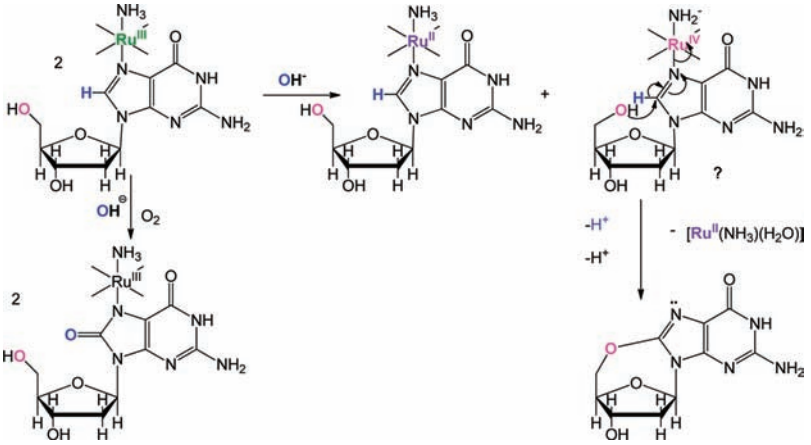

[a] It is noted that the $[Ru^{IV}(NH_3)_4(NH_2^-)(dGuo)]$ intermediate was not detected but deduced from the previous work.[5,6] And, the two-electron transfer from dGuo to Ru^{IV} scheme is also deduced by analogy with the $[Pt^{IV}$-3′-dGMP] work.[4b] There is no rationale for putting a NH_2^- ligand in the trans position.

It has been known that ammine(pyridine)ruthenium complexes such as $[Ru^{III}(NH_3)_5(py)]$[5] and *trans*-$[Ru^{III}(NH_3)_4(py)L]$ (L = Ino, Guo, dGuo, Gua, etc.)[6] disproportionate to the corresponding complexes of Ru^{II} and Ru^{IV}. Our results have shown that ammineruthenium complexes without pyridine can also undergo disproportionation reactions. The disproportionation of $[Ru^{III}(NH_3)_5(dGuo)]$ follows the same kinetic law as that of *trans*-$[Ru^{III}(NH_3)_4(py)(L)]$ series. But *trans*-$[Ru^{III}(NH_3)_4(py)(dGuo)]$ disproportionates approximately 6 times faster (k_1 = 6.4 M^{-1} s^{-1})[6a] than that of $[Ru^{III}(NH_3)_5(dGuo)]$ (k_1 = 1.0 ± 0.06 M^{-1} s^{-1}) due to the π accepting nature of the pyridine ligand stabilizing Ru^{II}. After disproportionation, *trans*-$[Ru^{III}(NH_3)_4(py)(dGuo)]$ undergoes hydrolysis of the glycosidic bond to produce *trans*-$[Ru^{III}(NH_3)_4(py)(Gua)]$ (Gua: guanine).[6] However, we did not observe $[Ru^{III}(NH_3)_5(Gua)]$, the product of glycosidic bond breakage from our $[Ru^{III}(NH_3)_5(dGuo)]$ in basic solution. Only when $[Ru^{III}(NH_3)_5(dGuo)]$ was in an acidic solution (pH 4.0), the hydrolyzed species, $[Ru^{III}(NH_3)_5(dGua)]$, was observed (Figure S2, Supporting Information). In a slightly acidic condition (pH 6.7) after 1 week of reaction, only cyclic-dGuo not $[Ru^{III}(NH_3)_5(dGua)]$ was observed (Figure S3, Supporting Information).

The deprotonation of an ammine was suggested to be the rate-determining step for the disproportionation by Clarke's group.[6] This is reasonable because it is known that the deprotonation of ammine in $[Ru^{III}(NH_3)_6]$ occurs in basic solution (pK_a = 13.1 ± 0.3),[9] and the disproportionation rate depends on the hydroxide concentration. The deprotonated ammine, NH_2^-, as a π donor stabilizes Ru^{IV}, which can explain why the *trans*-$[Ru^{III}(NH_3)_4(py)(Ino)]$ complex disproportionates 10 times faster than *trans*-$[Ru^{III}(NH_3)_4(py)(dGuo)]$. Because ammine in the former complex can deprotonate more favorably due to the low electron density of inosine compared to dGuo. Inosine does not have an electron-donating exoamine at C2, while dGuo does.[6b]

On the basis of these observations, we propose two $[Ru^{III}(NH_3)_5(dGuo)]$ molecules disproportionate to $[Ru^{II}(NH_3)_5(dGuo)]$ and $[Ru^{IV}(NH_3)_4(NH_2^-)(dGuo)]$ via deprotonation of ammine by OH^-. The cyclization was also observed to be accelerated by OH^-. The k_{cycle} values at 25 °C were determined to be 5.9 (±0.7) × 10^{-4} s^{-1} and 3.2 (±0.2) × 10^{-4} s^{-1} at pH 10.8 and 10.1, respectively. The calculated k_{obs} values of disproportionation using the linear equation in Figure 8 are 7.7 (±0.8) × 10^{-4} s^{-1} and 2.6 (±0.7) × 10^{-4} s^{-1} at pH 10.8 and 10.1, respectively. The k_{cycle} and k_{obs} values at each pH are in the same range of order of magnitude (±20%), suggesting that cyclization immediately follows disproportionation. This should produce a very short lifetime for the putative $[Ru^{IV}(NH_3)_4(NH_2^-)(dGuo)]$ intermediate. This may be the reason why there was no distinctive band due to $[Ru^{IV}(NH_3)_4(NH_2^-)(dGuo)]$, although a very broad band around 567 nm could be due to $[Ru^{IV}(NH_3)_4(NH_2^-)(dGuo)]$.

Therefore, we propose that cyclic-dGuo is originated from a short-lived $[Ru^{IV}(NH_3)_4(NH_2^-)(dGuo)]$. Similar to the $[Pt^{IV}(dach)(Cl^-)_3(3'$-dGMP)] (dach = diaminecyclohexyl) case,[4b] the 5′-OH attacks the highly polarized C8 of dGuo in $[Ru^{IV}(NH_3)_4(NH_2^-)(dGuo)]$ followed by a subsequent two-electron transfer from dGuo to Ru^{IV} to produce cyclic-dGuo and $[Ru^{II}]$. In the presence of O_2 and OH^-, on the other hand, OH^- attacks C8 followed by a one-electron transfer to Ru^{III} and another one-electron transfer to O_2, to produce $[Ru^{III}(NH_3)_5(8\text{-oxo-dGuo})]$.[3] The proposed mechanism is shown in Scheme 1.

CONCLUSION

We have demonstrated that a two-electron oxidation of G derivative can be achieved from a Ru^{III} complex without O_2. The identification of cyclic-dGuo along with the kinetic similarity between the productions of $[Ru^{II}(NH_3)_5(dGuo)]$ and cyclic-dGuo from $[Ru^{III}(NH_3)_5(dGuo)]$ led us to conclude that $[Ru^{III}(NH_3)_5(dGuo)]$ disproportionates to $[Ru^{II}(NH_3)_5(dGuo)]$ and $[Ru^{IV}(NH_3)_4(NH_2^-)(dGuo)]$, which is immediately followed by the production of cyclic-dGuo from $[Ru^{IV}(NH_3)_4(NH_2^-)(dGuo)]$ via a two-electron redox reaction assisted by an intramolecular nucleophile.

EXPERIMENTAL SECTION

Materials. $[Ru^{III}(NH_3)_5Cl]Cl_2$ (Ru^{III}) was purchased from Alfa Aesar, and deoxyguanosine (dGuo) was purchased from Sigma Aldrich. $H_2{}^{18}O$ was purchased from Isotopes, Inc. Mossy Zn was purchased from

dx.doi.org/10.1021/ic2003518 |*Inorg. Chem.* 2011, 50, 6567–6574

Acros Organics, and $HgCl_2$ was purchased from Fisher Scientific. All of the other chemicals were purchased from Sigma-Aldrich. All water was purified by a Hydro Picotech 2 purification system. Aqueous ammonium acetate solvent was prepared by diluting a stock solution of 1 M ammonium acetate (pH 4.2) to 0.01 M using water.

pH Measurements. An Orion Research Expandable Ion Analyzer EA 940 equipped with a Corning Semi-Micro electrode was used to measure the pH. Values in D_2O solutions were not corrected for the effect of deuterium on the electrode and were noted as pH*.

Synthesis of Zn/Hg Amalgam. Approximately 4 g of Mossy Zn and 0.3 g of $HgCl_2$ were mixed in 5 mL of water and 0.6 mL of concentrated HCl, and the mixture was shaken for at least 5 min. The liquid was decanted, and 0.6 mL of water and 3 mL of concentrated HCl were newly added to store the Zn/Hg amalgam until it was used for the synthesis reaction. But, it was never stored for more than a day.

Synthesis of $[Ru^{III}(NH_3)_5(dGuo)]$. $[Ru^{III}(NH_3)_5(dGuo)]$ was synthesized by mixing 10 mmol of $[Ru^{III}(NH_3)_5Cl]Cl_2$ (Ru^{III}) with a 10% excess of dGuo (11 mmol) in 4 mL of water to ensure that Ru^{III} was reacted to completion. The pH of the reaction solution was adjusted to less than pH 3.5 using 3 M HCl. Zn/Hg amalgam was added, and N_2 was bubbled through the solution for approximately 45 min to reduce Ru^{III} to Ru^{II}, which then bound to dGuo. When the mixture turned greenish-yellow, the solution was removed from the Zn/Hg amalgam by decanting it into a new reaction tube. Then, O_2 was bubbled through the greenish-yellow solution for over an hour to oxidize $[Ru^{II}(NH_3)_5(dGuo)]$ to $[Ru^{III}(NH_3)_5(dGuo)]$, which yielded a purple solution. The product was characterized by HPLC and LC/MS (m/z 455.0). The experimental MS spectrum shows exactly the same isotopic progression as the theoretical MS spectrum (Figure S4, Supporting Information).

Redox Reaction of $[Ru^{III}$-dGuo] in Basic Solution. *Under O_2.* The pH of the reaction solution from the synthesis of $[Ru^{III}(NH_3)_5(dGuo)]$ (2−4 mL) was raised to above pH 11 using 6 M NaOH, which changed the color of the solution from purple to blue. O_2 was bubbled through the solution overnight, which yielded a black solution with a black precipitate. The resulting products in the reaction solution were characterized by HPLC and LC/MS.

Under Ar. The reaction solution from the synthesis of $[Ru^{III}(NH_3)_5(dGuo)]$ (2−4 mL) and the 6 M NaOH solution used for adjusting pH were purged with Ar (Airgas, 99.997% pure, O_2 < 5 ppm) for several minutes to remove any O_2 present in these solutions. Then, while under Ar, the pH of the reaction solution from the synthesis of $[Ru^{III}(NH_3)_5(dGuo)]$ was raised to above pH 11, which changed the color of the solution from purple to blue. Ar was bubbled through the solution for several days, yielding a black solution with a black precipitate. The resulting products in the solution were characterized by HPLC and LC/MS.

HPLC. HPLC was used to analyze the composition of reaction mixtures and to collect specific fractions. Analytical HPLC chromatograms were obtained using a Waters Alliance 2695 liquid chromatograph, which was fitted with a reverse-phase Waters Atlantis dC18 column (250 mm × 4.6 mm, 5 μm) and a Waters 2996 photodiode array detector. The photodiode array detector was set to 254 nm. Isocratic elutions were used with 97% 10 mM ammonium acetate (pH 4.2) and 3% acetonitrile. All solutions were filtered through a syringe-driven filter (Millex-LH 0.45 μm pore size) prior to injection.

Mass Spectrometry. Liquid chromatography coupled with mass spectrometry (LC/MS) was used to verify the identity of synthesized adducts and reaction products. LC/MS analyses were conducted using an Agilent 1100 Series LC with an XCT Plus LC/MSD trap. The LC was equipped with a photodiode array detector and an Eclipse XDB-C8 Column (4.6 mm × 150 mm, 5 μm) and was run using a gradient elution at a 0.5 mL/min flow rate, beginning with 0.1% formic acid in water for 5 min, followed by a steady gradient to 80:20 0.1% formic acid to isopropyl alcohol for 5 min, and then ending with isocratic 80:20 0.1% formic acid to isopropyl alcohol until 25 min was reached. For the MS component, an ion trap mass spectrometer was set to scan from 50 to 2200 m/z detecting positive ions with electrospray ionization mass spectrometry (ESI-MS), and no peaks were excluded from MS^2 analysis. For tuning, the nebulizer was set to 50 psi, the dry temperature to 365 °C, and the dry gas (helium) flow to 9 L/min. All solutions were filtered through a syringe-driven filter (Millex-LH 0.45 μm pore size) prior to injection.

^{1}H NMR Spectroscopy. NMR spectra were recorded on a Bruker NMR spectrometer equipped with a broad band inverse tunable probe operating at 400.13 MHz for ^{1}H. Chemical shifts for ^{1}H were adjusted relative to tetramethylsilane (TMS). Samples were prepared in D_2O, and the residual water signal was further suppressed by the watergate pulse sequence.[10]

UV−Vis Spectroscopy. UV−vis was used to characterize $[Ru^{II}(NH_3)_5(dGuo)]$ and $[Ru^{III}(NH_3)_5(dGuo)]$ during and after the synthesis reaction, respectively, and also to monitor the formation of $[Ru^{II}(NH_3)_5(dGuo)]$ from $[Ru^{III}(NH_3)_5(dGuo)]$. Reactions were generally diluted with water prior to obtaining spectra, but more focus was given to being able to detect the absorbance in the 350−800 nm region clearly. Data were collected on a Cary 4000 spectrophotometer from 200 to 800 nm. Spectra were obtained in 1 cm quartz microcuvettes and were baseline-corrected using a water standard.

Kinetic Studies. Reaction rates under Ar were monitored using an airtight cuvette (Sterna Cells, Inc.) via UV−vis spectroscopy. Spectra were collected on a Cary 4000 spectrophotometer using kinetic assay software. The reaction was monitored as a function of pH by following the increase in absorbance at 354 nm due to $[Ru^{II}(dGuo)]$. The data were then fitted to a first-order kinetics expression.

■ ASSOCIATED CONTENT

Supporting Information. The UV−vis spectra of $[Ru^{II}(NH_3)_5(dGuo)]$ at pH 9.0 and t = 0 (Figure S1). Production of $[Ru^{III}(NH_3)_5(dGua)]$ from $[Ru^{III}(NH_3)_5(dGuo)]$ at pH 4.0 (Figure S2). Production of cyclic-dGuo from $[Ru^{III}(NH_3)_5(dGuo)]$ after 1 week at pH 6.7 (Figure S3). MS spectra of experimental and theoretical $[Ru^{III}(NH_3)_5(dGuo)]$ (Figure S4). This information is available free of charge via the Internet at http://pubs.acs.org/.

■ AUTHOR INFORMATION

Corresponding Author
*E-mail: choi@middlebury.edu.

■ ACKNOWLEDGMENT

This work was supported by the National Science Foundation (Grant CHE-0450060 and CHE-0848072) and Arnold and Mabel Beckman Foundation. We thank Edith Larya-Walker for collecting cyclic-dGuo from the HPLC.

■ REFERENCES

(1) (a) Sies, H. *Oxidative Stress, Oxidants and Antioxidants*; Academic Press: New York, 1991. (b) Marnett, L. J.; Burcham, P. C. *Chem. Res. Toxicol.* **1993**, *6*, 771–785.(c) Cadet, J. In *DNA Adducts: Identification and Biological Significance*; Hemminki, J., Dipple, A., Shuker, D. G. E., Kadlubar, F. F., Segerback, D., Bartsch, H., Eds.; IARC Sci. Pub.: Lyon, france, 1994; Vol. 125, pp 245−276.

(2) (a) Burrows, C. J.; Muller, J. G. *Chem. Rev.* **1998**, *98*, 1109–1151. (b) Pyle, A. M.; Barton, J. K. *Prog. Inorg. Chem: Bioinorg. Chem.* **1990**, *38*, 413–475. (c) Chow, C. S.; Barton, J. K. *Methods Enzymol.* **1992**, *212*, 219–242. (d) Pratviel, G.; Meunier, B. *Chem.—Eur. J.* **2006**, *12*, 6018–6030.

(3) (a) Gariepy, K. C.; Curtin, M. A.; Clarke, M. J. *J. Am. Chem. Soc.* **1989**, *111*, 4947–4952. (b) Rodriguez-Bailey, V. M.; LaChance-Galang, K. J.; Doan, P. E.; Clarke, M. J. *Inorg. Chem.* **1997**, *36*, 1873–1883.

(4) (a) Choi, S.; Cooley, R. B.; Hakemian, A. S.; Larrabee, Y. C.; Bunt, R. C.; Maupaus, S. D.; Muller, J. G.; Burrows, C. J. *J. Am. Chem. Soc.* **2004**, *126*, 591–598. (b) Choi, S.; Cooley, R. B.; Voutchkova, A.; Leung, C. H.; Vastag, L.; Knowles, D. E. *J. Am. Chem. Soc.* **2005**, *127*, 1773–1781. (c) Choi, S.; Personick, M. L.; Bogart, J. A.; Ryu, D. W.; Redman, R. M.; Laryea-Walker, E. *Dalton Trans.* **2011**, *40*, 2888–2897.

(5) Rudd, D. F.; Taube, H. *Inorg. Chem.* **1971**, *10*, 1543–1544.

(6) (a) LaChance-Galang, K. J.; Zhao, M; Clarke, M. J. *Inorg. Chem.* **1996**, *35*, 6021–6026. (b) Zhao, M.; Clarke, M. J. *J. Biol. Inorg. Chem.* **1999**, *4*, 318–324. (c) Zhao, M.; Clarke, M. J. *J. Biol. Inorg. Chem.* **1999**, *4*, 325–340.

(7) Guengerich, F. P.; Mundkowski, R. G.; Voehler, M.; Kadlubar, F. F. *Chem. Res. Toxicol.* **1999**, *12*, 906–916.

(8) Silverstein, R. M.; Bassler, G. C.; Morrill, T. C. *Spectrometetric Identification of Organic Compounds*, 5th ed.; John Wiley & Sons, Inc.: New York, 1999; pp 196−197.

(9) Waysbort, D.; Navon, G. *Inorg. Chem.* **1979**, *18*, 9–13.

(10) Trimble, L. A.; Bernstein, M. A. *J. Magn. Reson. Ser. B* **1994**, *105*, 67–72.